Eddy Dissipation Combustion Modeling of Turbulent Reacting Flow

Majid Almas[1,2,*]

[1]*Department of Mechanical and Materials Engineering, Florida International University, Miami, FL 33199, USA*

[2]*Department of Marine engineering, King AbdulAziz University, 21589, Saudi Arabia*

Abstract: In this paper specious transport and gaseous combustion have been modeled numerically using computational fluid dynamics method. A cylindrical combustor burning methane (CH_4) in air is studied using the eddy-dissipation model. Eddy dissipation combustion model has been coupled with the standard $k-\varepsilon$ model to simulate this highly complex turbulent reactive fluid flow field. Effects of air and fuel velocities have been investigated on the reactant mass fractions, temperature and velocity profiles and NO_X production.

Keywords: Gaseous combustion, eddy dissipation, specious transport, NO_X production.

1. INTRODUCTION

Combustion is an interdisciplinary topic which combines the most sophisticated phenomena of fluid dynamics and chemical reactions. Combustion involves many complex phenomena, such as turbulence, recirculation, mixing, fuel chemistry, turbulence–chemistry interaction, heat and mass transfer. The chemical reaction takes place in a turbulent environment where the highly unsteady fluid motions of a wide range of length and time scales are present. Turbulence–combustion [1] and [2] interaction is one of the most complicated products of this combination. Study of turbulence effect on chemical reaction is challenging in many aspects. Comprehending of the complex effects of a macro level phenomenon (turbulence) on a molecular lever phenomenon (chemical reaction) is the main challenge Natural gas offers an interesting alternative to traditional fuels to reduce pollutant emissions and to lower the energy dependence of road vehicles on oil. The addition of hydrogen to natural gas has even more advantages in terms of pollutant reduction, thermal efficiency, and combustion stability allowing some combustion systems to operate with lean fuel mixtures. Hydrogen offers high flame speeds, a wide flammability range [3-5], low minimum ignition energy and no emissions of HC or CO_2 [6, 7]. It is actually considered as one of the most promising alternative fuels for future engines. Combination of hydrogen with other fuels is one effective approach to use of hydrogen for clean combustion. Recent studies on internal combustion engines with hydrogen-enriched fuels showed that hydrogen addition could increase thermal efficiency, improve lean burn capability and mitigate the global warming problem [6, 8-10]. Due to lower temperatures of very lean flames, NOx emissions also decreased significantly [11]. In this study a cylindrical combustor burning methane in air is studied using the eddy-dissipation model. Eddy dissipation combustion model has been used for modeling the combustion and $k-\varepsilon$ model has been applied for solving the turbulent flow. Effects of air and fuel velocities and their temperatures have been studied on temperature and NO emission.

2. PROBLEM DEFINITION

The cylindrical combustor considered in this paper is shown in Figure **1**. The flame considered is a turbulent diffusion flame. A small nozzle in the center of the combustor introduces methane at 80m/s. Ambient air enters the combustor coaxially at 0.5m/s. The overall equivalence ratio is approximately 0.76 (approximately 28% excess air). The high-speed methane jet initially expands with little interference from the outer wall, and entrains and mixes with the low-speed air. The Reynolds number based on the methane jet diameter is approximately 5.7×10^{-3}. Structure mesh has been used with the accumulation of the grids near the bottom wall. The convergence criteria for momentum and continuity is $10e^{-3}$ and $10e^{-6}$ is for energy and turbulence equations. Second order upwind for momentum and for kinetic and dissipation first order upwind has been used.

3. REACTION EQUATION

In this work the generalized eddy-dissipation is modeled to analyze the methane-air combustion

*Address correspondence to this author at the Department of Mechanical and Materials Engineering, Florida International University, Miami, FL 33199, USA; Tel: (305) 348-1932; Fax: (305) 348-2569; E-mail: malma016@fiu.edu

E-ISSN: 2409-5761/16

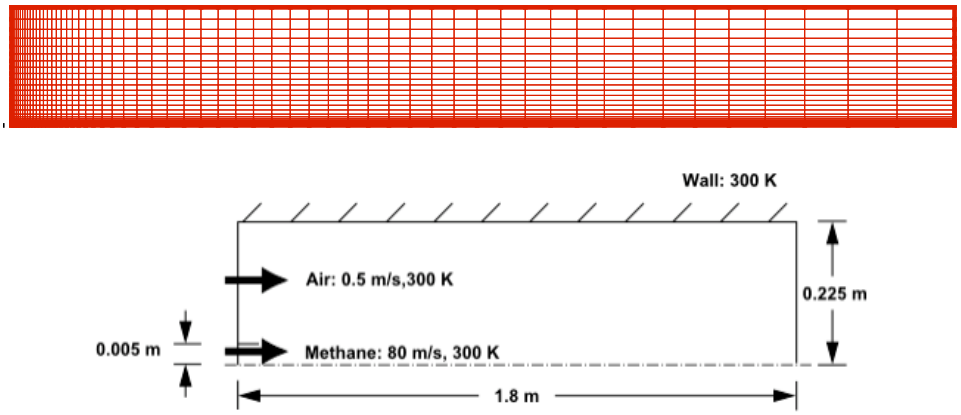

Figure 1: Geometry and grid generation of the problem.

system. The combustion is modeled using a global one-step reaction mechanism, assuming complete conversion of the fuel to CO_2 and H_2O. The reaction equation is;

$$CH_4 + 2O_2 \rightarrow CO_2 + 2H_2O \quad (1)$$

The reaction rate is determined assuming that turbulent mixing is the rate-limiting process, with the turbulence-

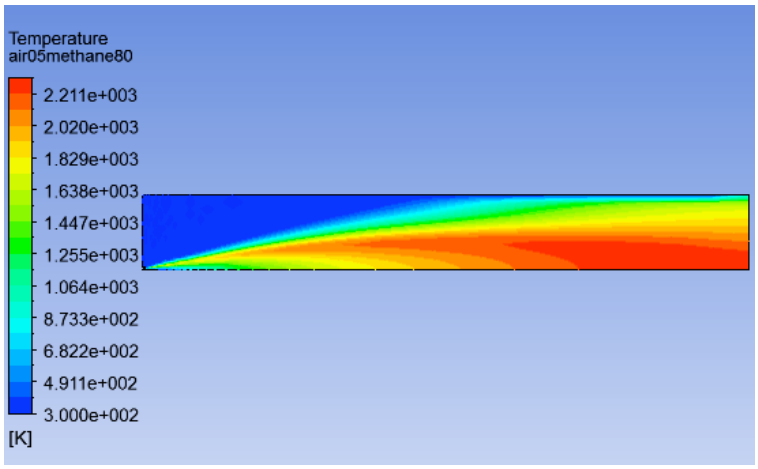

Figure 2: Temperature contour for inlet velocities of air at 0.5(m/s) and methane at 80(m/s).

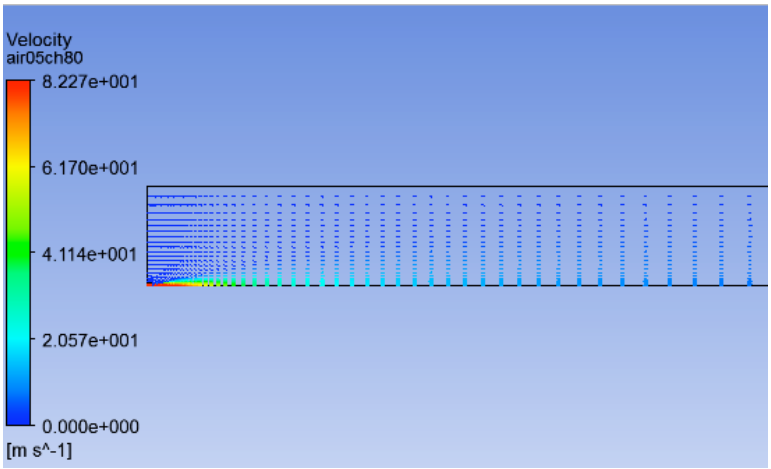

Figure 3: Velocity magnitude for inlet velocities of air at 0.5(m/s) and methane at 80(m/s).

chemistry interaction modeled using the eddy-dissipation model.

4. RESULTS AND DISCUSSIONS

Figure **2** shows the contours of temperature for inlet velocities of air and methane at 0.5 and 80m/s respectively. As can be seen the temperature increases as the two reactants mix and the combustion occurs. This value increases up to 2211K from its primary values for both air and methane at 300K.

Velocity magnitude for inlet velocities of air at 0.5 (m/s) and methane at 80 (m/s) is shown in Figure **3**. As expected the velocity has its maximum value at the inlet where the fluids are injected to the domain.

Figure **4** displays the CO_2 mass fraction for inlet velocities of air and methane at 0.5 and 80m/s respectively. As can be seen from Eq. (1), CO_2 is one of the products of the combustion on the right hand side of the equation. As shown in the figure, the concentration of CO_2 is high when the inlet reactants mix and combustion happens. The CO_2 mass fraction value is 0.146 when combustion occurs.

Figure **5** depicts the H_2O mass fraction for inlet velocities of air and methane at 0.5 and 80m/s respectively. H_2O is also one of the combustion products as seen in Eq. (1). As shown in the figure, the concentration of H_2O is at its highest after combustion occurs. Mixing of inlet reactants produces H_2O mass fraction of 0.119. As seen H_2O concentration is at its

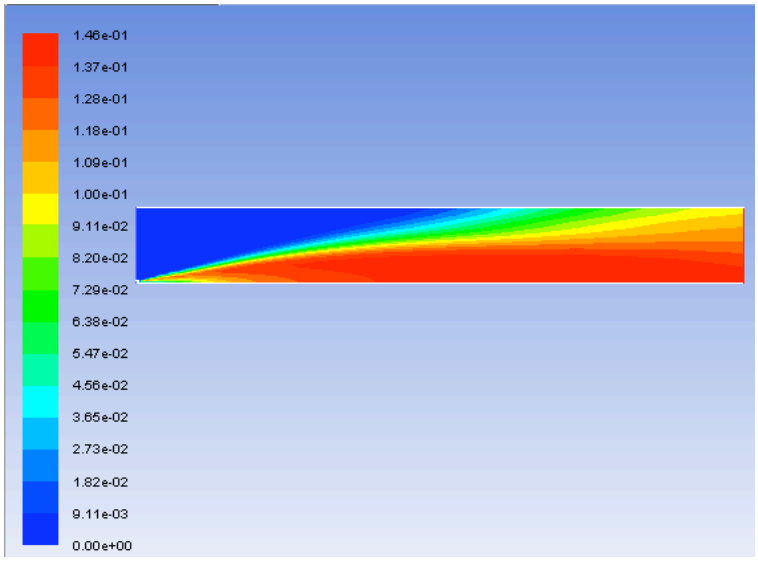

Figure 4: CO_2 mass fraction for inlet velocities of air at 0.5(m/s) and methane at 80(m/s).

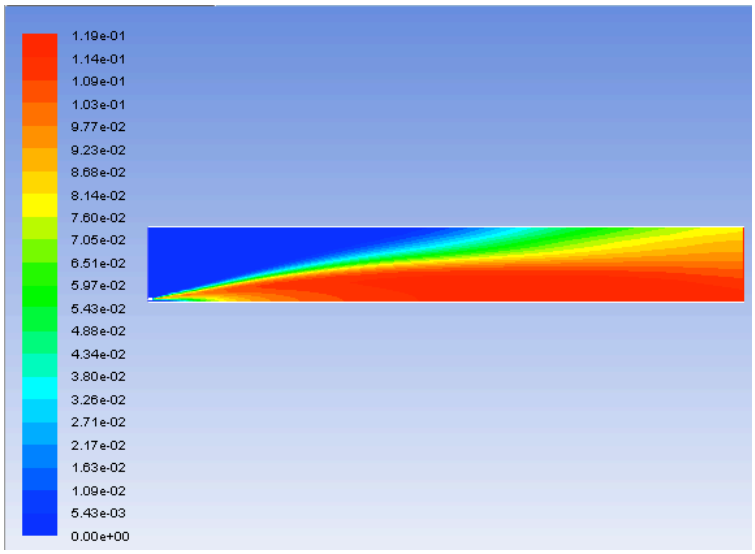

Figure 5: H_2O mass fraction for inlet velocities of air at 0.5(m/s) and methane at 80(m/s).

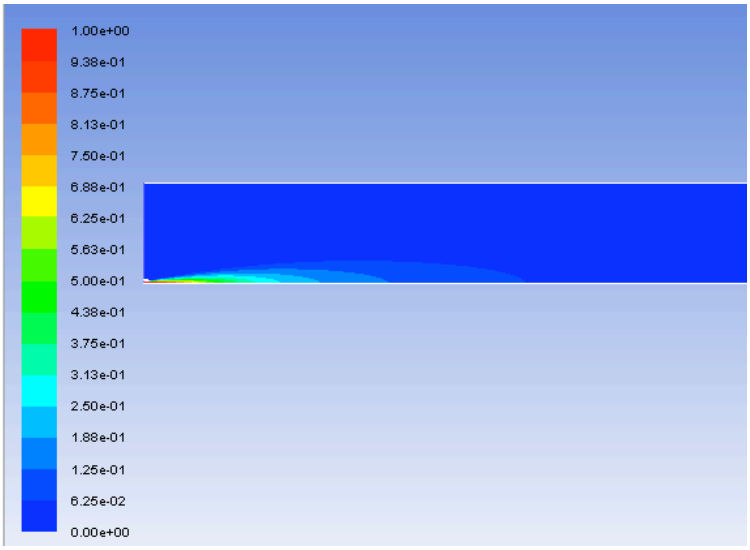

Figure 6: CH_4 mass fraction for inlet velocities of air at 0.5(m/s) and methane at 80(m/s).

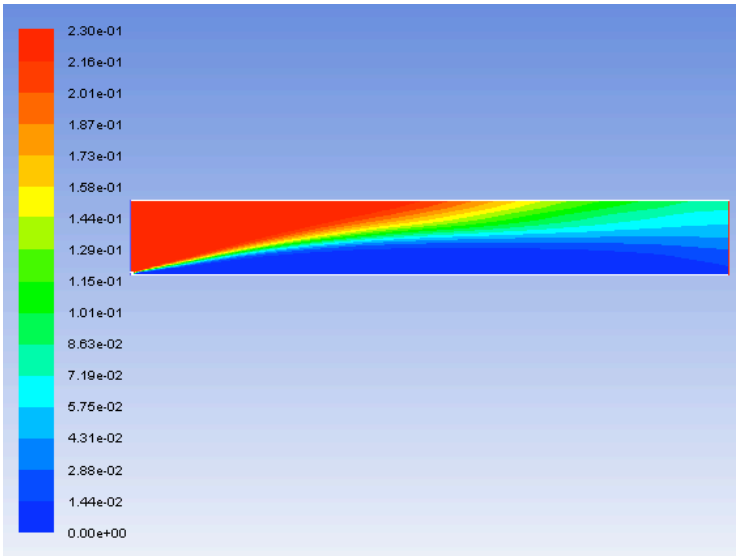

Figure 7: O_2 mass fraction for inlet velocities of air at 0.5(m/s) and methane at 80(m/s).

highest close to the bottom wall of cylinder where the methane injects to the chamber and mix with the inlet air.

Figure **6** presents the CH_4 mass fraction for inlet velocities of air and methane at 0.5 and 80m/s respectively. As expected the CH_4 has its maximum value at the inlet where the fluids are injected to the domain. Methane as one of the inlet reactants injected in the cylindrical chamber has its highest concentration on near the bottom surface where it is injected to the domain. At the inlet methane has its maximum value which reduces as it moves downstream of the domain as it consumes when the combustion occurs.

Figure **7** demonstrates the O_2 mass fraction for inlet velocities of air and methane at 0.5 and 80m/s respectively. As seen the O_2 has its maximum value at the inlet where the fluids are injected to the domain. Air as one of the inlet reactants injected in the cylindrical chamber has its highest concentration on near the top wall where it is injected. At the inlet O_2 has its maximum value which reduces as it moves down-stream of the domain as it consumes when the combustion occurs.

Figure **8** shows the NO mass fraction for inlet velocities of air and methane at 0.5 and 80m/s respectively. As seen the mass fraction of NO is very low in the region near the inlet where the inlet reactants start to mix. This value increases as more mixing happens and combustion gets complete. After complete combustion the concentration of NO grows

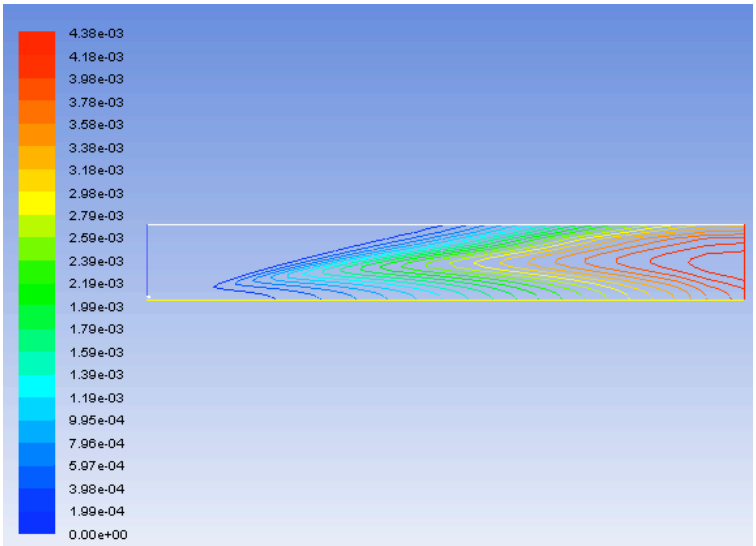

Figure 8: NO mass fraction for inlet velocities of air at 0.5(m/s) and methane at 80(m/s).

and this value continue increasing toward the outlet of the chamber.

Figure **9** displays the temperature profile for inlet velocities of air at 0.5, 0.9 and 1.4(m/s) and methane at 80(m/s). Here the effects of different air velocities with constant methane velocity have been studied on outlet temperature at the exit of the chamber. As shown the temperature reduces from 1900 to 1300 and 900K as the inlet air velocity increases from its primary value of 0.5 to 0.9 and 1.4m/s respectively.

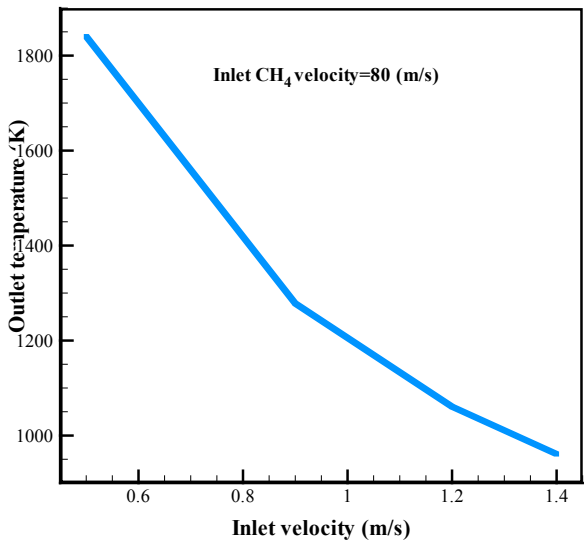

Figure 9: Temperature profile for inlet velocities of air at 0.5, 0.9 and 1.4(m/s) and methane at 80(m/s).

Figure **10** demonstrates the velocity profile for inlet velocities of air at 0.5, 0.9 and 1.4(m/s) and methane at 80(m/s). Here the effects of different air velocities with constant methane velocity have been studied on outlet velocity at the exit of the chamber. As shown the velocity values increase from 3.4 to 4 and 4.4m/s as the inlet air velocity increases from its primary value of 0.5 to 0.9 and 1.4m/s respectively.

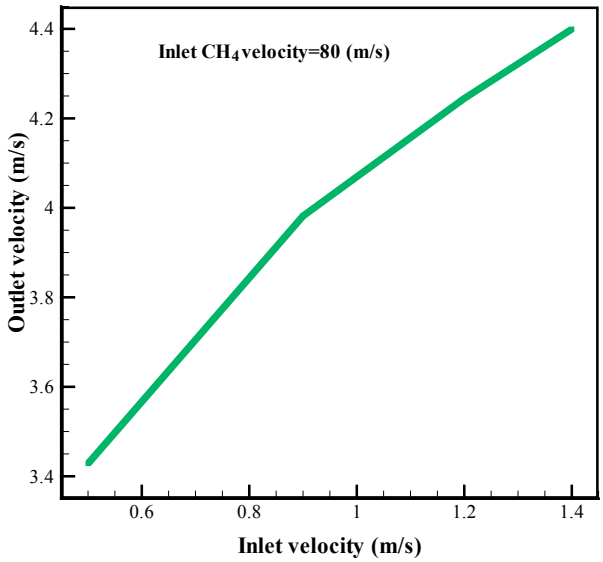

Figure 10: Velocity profile for inlet velocities of air at 0.5(m/s) and methane at 80(m/s).

Figure **11** depicts the NO mass fraction for inlet velocities of air at 0.5, 0.9 and 1.4 (m/s) and methane at 80(m/s). Here the effects of different air velocities with constant methane velocity have been studied on NO_x concentration. As shown the NO_x mass fraction decreases from 0.004 to 0.0034 and 0.0026m/s as the inlet air velocity increases from its primary value of 0.5 to 0.9 and 1.4m/s respectively.

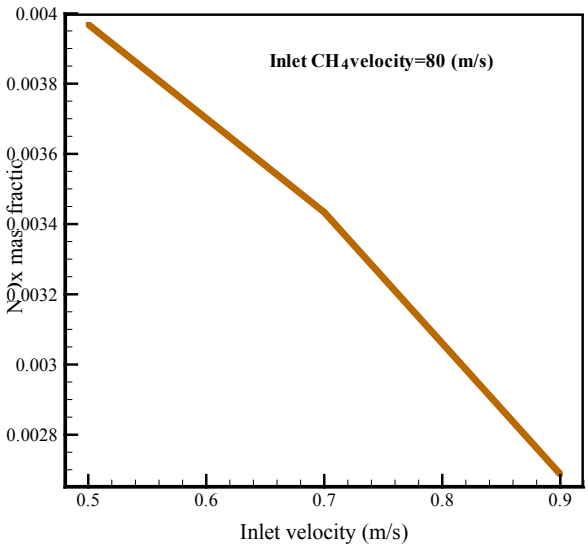

Figure 11: NO mass fraction for inlet velocities of air at 0.5, 0.7 and 0.9(m/s) and methane at 80(m/s).

Figure **12** shows Temperature profile for inlet velocities of methane at 80, 110, 160(m/s) and air at 0.5(m/s). Here the effects of different methane velocities with constant air velocity have been studied on outlet temperature at the exit of the chamber. As shown the outlet temperature increases from 1850K to 2125K for inlet methane velocities of 80m/s and 110m/s respectively and this value drops to almost its initial value of 1850K at velocity of 160m/s.

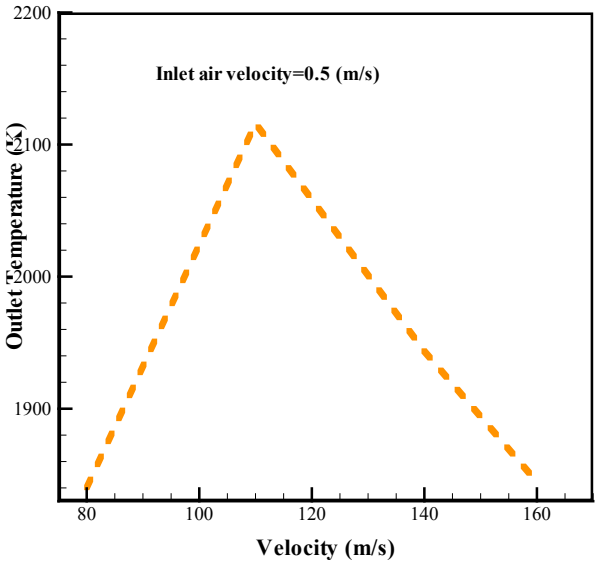

Figure 12: Temperature profile for inlet velocities of methane at 80, 110, 160(m/s) and air at 0.5(m/s).

Figure **13** depicts the velocity profile for inlet velocities of methane at 80, 110, 160 (m/s) and air at 0.5 (m/s). Here the effects of different methane velocities with constant air velocity have been studied on outlet velocity at the exit of the chamber. The outlet velocity increases from 3.4 to 4.15m/s for inlet methane velocities of 80m/s and 110m/s respectively. This value decreases to 3.8m/s at velocity of 160m/s.

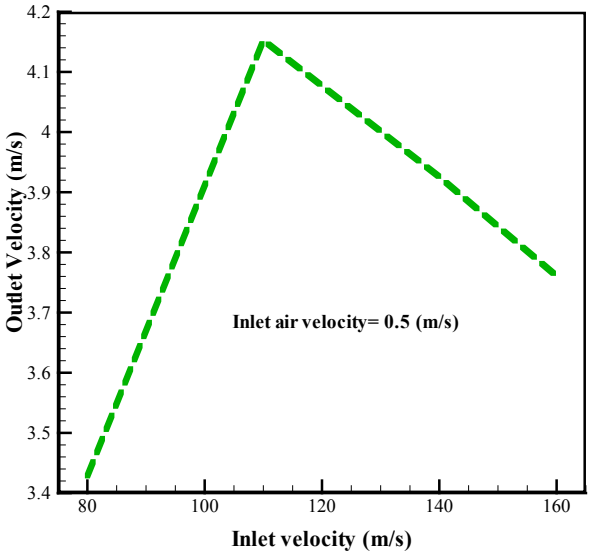

Figure 13: Velocity profile for inlet velocities of methane at 80, 110, 160(m/s) and air at 0.5(m/s).

Figure **14** shows the NO mass fraction for inlet velocities of air at 0.5, 0.9 and 1.4(m/s) and methane at 80(m/s). Here the effects of different methane velocities with constant air velocity have been studied on NO_x concentration. As shown the NO_x mass fraction decreases from 0.004 to 0.0018 and 0.00025 as the inlet air velocity increases from its primary value of 80 to 110 and 160m/s respectively.

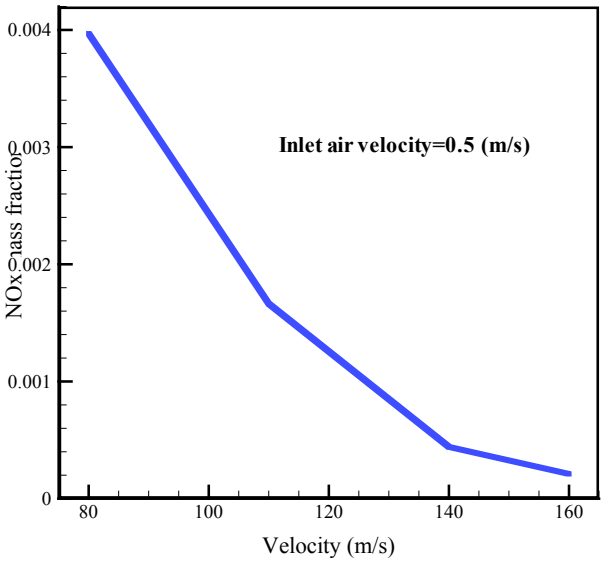

Figure 14: NO mass fraction for inlet velocities of air at 0.5, 0.7 and 0.9(m/s) and methane at 80(m/s).

CONCLUSIONS

In this study a cylindrical combustor burning methane in air is studied using the eddy-dissipation model. Eddy dissipation combustion model has been used for modeling the combustion and $k-\varepsilon$ model [2] has been applied for solving the turbulent flow. Effects of air and fuel velocities and their temperatures have been studied on temperature and NO emission. The numerical results have been shown and described through graphs. The numerical results show that NO_x mass fraction decreases as both velocities of air and methane increase. And also the outlet temperature in both cases decrease as the inlet reactant velocities enhance. Results also revealed that the outlet velocities increase in both cases as the inlet reactant velocities increase.

ACKNOWLEDGMENTS

The author would like to thank both the Saudi Arabian Cultural Mission in Washington D.C. and King Abdulaziz University in Jeddah, KSA for their support.

REFERENCES

[1] Agrawal GK and Suman Chakraborty SK. Some Heat transfer characteristics of premixed flame impinging upwards to plane surfaces inclined with the flame jet axis. Int J Heat Mass Transf 2010; 53: 1899-1907. http://dx.doi.org/10.1016/j.ijheatmasstransfer.2009.12.068

[2] Ghasemi E, McEligot DM, Nolan KP, Crepeau J, Tokuhiro A and Budwig RS. Entropy generation in a transitional boundary layer region under the influence of free stream turbulence using transitional RANS models and DNS. Int Commu heat Mass transfer 2013; 41: 10-16. http://dx.doi.org/10.1016/j.icheatmasstransfer.2012.11.005

[3] Wang J, Huang Z, Miao H, Wang X and Jiang D. Characteristics of direct injection combustion fuelled by natural gas–hydrogen mixtures using a constant volume vessel. Int J Hydrogen Energy 2008; 33: 1947-1956. http://dx.doi.org/10.1016/j.ijhydene.2008.01.007

[4] Ilbas M, Crayford AP, Yilmaz I, Bowen PJ and Syred N. Laminar-burning velocities of hydrogen–air and hydrogen–methane–air mixtures: an experimental study. Int J Hydrogen Energy 2006; 31: 1768-1779. http://dx.doi.org/10.1016/j.ijhydene.2005.12.007

[5] Wierzba I and Wang Q. The flammability limits of H2–CO–CH4 mixtures in air at elevated temperatures. Int J Hydrogen Energy 2006; 31: 485-489. http://dx.doi.org/10.1016/j.ijhydene.2005.04.022

[6] do Sacramento EM, de Lima LC, Oliveira CJ and Veziroglu TN. A hydrogen energy system and prospects for reducing emissions of fossil fuels pollutants in the Ceará state-Brazil. Int J Hydrogen Energy 2008; 33: 2132-2137. http://dx.doi.org/10.1016/j.ijhydene.2008.02.018

[7] Granovskii M, Dincer I and Rosen MA. Greenhouse gas emissions reduction by use of wind and solar energies for hydrogen and electricity production: economic factors. Int J Hydrogen Energy 2007; 23: 927-931. http://dx.doi.org/10.1016/j.ijhydene.2006.09.029

[8] Van Blarigan P and Keller JO. A hydrogen fuelled internal combustion engine designed for single speed/power operation. Int J Hydrogen Energy 1998; 23: 603-609. http://dx.doi.org/10.1016/S0360-3199(97)00100-6

[9] Wang J, Huang Z, Fang Y, Liu B, Zeng K, Miao H, et al. Combustion behaviors of a direct-injection engine operating on various fractions of natural gas–hydrogen blends. Int J Hydrogen Energy 2007; 32: 3555-564. http://dx.doi.org/10.1016/j.ijhydene.2007.03.011

[10] Saravanan N and Nagarajan G. An experimental investigation of hydrogen-enriched air induction in a diesel engine system. Int J Hydrogen Energy 2008; 33: 1769-1775. http://dx.doi.org/10.1016/j.ijhydene.2007.12.065

[11] Coppens FHV, De Ruyck J and Konnov AA. Effects of hydrogen enrichment on adiabatic burning velocity and NO formation in methane + air flames. Exp Thermal Fluid Sci 2007; 31: 437-444. http://dx.doi.org/10.1016/j.expthermflusci.2006.04.012

Received on 09-06-2016 Accepted on 18-06-2016 Published on 31-07-2016

DOI: http://dx.doi.org/10.15377/2409-5761.2016.03.01.9